8-9-2017

Influence of Adsorbed and Nonadsorbed Polymer Additives on The Viscosity of Magnesium Oxide Suspensions

Lisa R. Murray

Jason E Bice

Emily G. Soltys

Christopher Perge

Sebastien Manneville

See next page for additional authors

Authors

Lisa R. Murray, Jason E Bice, Emily G. Soltys, Christopher Perge, Sebastien Manneville, and Kendra Erk

Title: Influence of adsorbed and non-adsorbed polymer additives on the viscosity of magnesium oxide suspensions

Authors:

Lisa R. Murray,[a*] , Jason E. Bice[a], Emily G. Soltys[a] , Christophe Perge[b] , Sébastien Manneville[b], Kendra A. Erk[a]

[a*] Currently at Anton Paar USA, 10215 Timber Ridge Dr., Ashland, VA 23005, Lisa.Murray@Anton-Paar.com

[a] School of Materials Engineering, Purdue University, 701 West Stadium Ave., West Lafayette, IN, USA 47907, bicej@purdue.edu

[a] School of Materials Engineering, Purdue University, 701 West Stadium Ave., West Lafayette, IN, USA 47907, soltys@purdue.edu

[b] Univ Lyon, Ens de Lyon, Univ Claude Bernard, CNRS, Laboratoire de Physique, F-69342 Lyon, France

[b] Univ Lyon, Ens de Lyon, Univ Claude Bernard, CNRS, Laboratoire de Physique, F-69342 Lyon, France, sebastien.manneville@ens-lyon.fr

[a] School of Materials Engineering, Purdue University, 701 West Stadium Ave., West Lafayette, IN, USA 47907, Corresponding author: erk@purdue.edu

ABSTRACT

Adsorbed-polymer additives have been employed to reduce water content and improve cement workability through lowering viscosity, but the influence of over-dosage and the presence of non-adsorbed chains have yet to be fully understood. Model magnesium oxide (MgO) suspensions were used to investigate the potential processing effect of "free" chain concentration on cementitious mixtures. The rheological impact of the free chains was measured through incorporation of non-adsorbing poly(ethylene glycol) (PEG) to suspensions stabilized with an adsorbed comb-polymer superplasticizer. Analyses of the rheological data, that showed viscosity-increases and viscosity-reduction due to free PEG concentrations revealed a transition from depletion flocculation to depletion stabilization that contributed to the flow properties of the suspensions. The viscosity-reduction observed for high concentrations of free chains may be useful for improved mixing of cements with free polymer in addition to the adsorbed polycarboxylate ether-based superplasticizer (PCE). Additionally, the influence of free PEG on the macroscale flow behavior was also examined through local velocity measurements under shear.

INTRODUCTION

Magnesium oxide suspensions have been used as a model system for cementitious pastes due to their similar flow properties and polymer adsorption characteristics [1–5]. Cement processing can be examined through the study of magnesium oxide suspensions' response to mixing and pouring without consideration of the later impact of hydration reactions[2,4,6]. Therefore, the flow behavior of the suspensions can be investigated through rheometry and polymer superplasticizers as an analog for cement processing.

Adsorbed polymer additives are commonly used in cements and other concentrated suspensions to adjust the flow properties and induce dispersion. A particular class of polymer additives called superplasticizers employs comb-polymers to electrostatically adsorb to cement particles through an anionic main-chain with neutral side-chains emerging into the solution. As long as the main-chain of the superplasticizer is adsorbed, the side-chains are capable of sterically stabilizing the particle and thus offer a simple method for particle dispersion [2,8–11]. Often viscosity reduction results from the use of superplasticizers which promotes ease of workability for handling and placing concrete [3]. However, literature has reported that the presence of non-adsorbed superplasticizers may interfere with the fluidity of the cement and thus disrupt the workability [12]. Non-adsorbed polymer chains in cements pose both an academic and industrial challenge due to the complexity of the particle-polymer interactions and their role in processing.

Viscosity increases are often attributed to over-dosage of superplasticizers in cementitious pastes [13,14], but few studies have investigated the role of free polymer among adsorbed polymer-particle suspensions. Furthermore, experimentation on aggregation is common for nano-scale colloids [15–18] but lacking in the micro-level for industrial pastes such as cements and slurries. Depletion of free chains in cement is often acknowledged but not fully considered [9], furthering the outlook that non-adsorbed polymer should be avoided or disregarded [13]. Herein free, non-adsorbed polymer is included with the adsorbed PCE to elucidate the mechanisms for viscosity alterations in model magnesium oxide (MgO) suspensions. In this paper, comparisons are made between suspensions containing free chains with and without adsorbed PEG based on the flow behaviors demonstrated by viscosity curves (shear ramp), start-up tests, and creep measurements. Three rheological regimes were found as the free chain concentration increased: depletion aggregation, depletion transition, and depletion stabilization. Based on ultrasonic velocimetry under shear, the free polymer was further shown to significantly affect the local flow behavior by promoting plug flow and strong wall slip. In this way free polymer is shown to work as a dispersion stabilizer at high concentrations through lubrication and osmotic pressure, which brings a new approach to viscosity-reduction for model cementitious suspensions.

MATERIALS AND METHODS

Materials

MgO particles were obtained from Martin Marietta Magnesia Specialties (MagChem P98 pulverized). Previous characterization of the MgO particles revealed the average particle size to be ~4 μm with a range of sizes between 0.5 and 40 μm [19]. ADVA 190 (Grace Construction), a commercial water-reducing PCE used in Portland cements, was applied as an additive for MgO suspensions. Previous work delineated the chemical structure of comb-polymer, which consists of ~5,000 g/mol poly(acrylic acid) (PAA) and ~15 1,000 g/mol grafted poly(ethylene oxide) (PEO) side-chains (PAA-PEO) [19,20]. PAA-PEO was dialyzed prior to use in order to remove any low molecular weight species [19]. The free, non-adsorbing polymer PEG of molecular weight 1,000 g/mol was obtained from Sigma Aldrich and used without further purification.

Suspension Fabrication

MgO suspensions were assembled by first dissolving the commercial PAA-PEO comb-polymer and PEG in water by stirring for 30 minutes. Different weight percentages of the PEG were tested by weight of the comb-polymer. To match industrial concentrations of additives in cements, the PAA-PEO concentration was 18 mg/mL. Further, several (0, 10, 20, 30, 40, and 50 w/w) weight % free PEG chains by weight of the PAA-PEO comb-polymer were considered, to examine the shear response with a small amount of non-adsorbed polymer. MgO powder was added gradually while stirring the suspension. Suspensions were sonicated for 5 minutes after fabrication, stirred overnight, and then sonicated again before testing. The water to MgO weight ratio was kept at 0.33 to simulate the concentrated particle loadings of high-strength cements [21]. Given the density of MgO is 3.58 g/cm^3 and ignoring the effect of polymer on the effective volume fraction, this corresponds to a solid volume fraction of 0.42.

The amount of free PEG among the particles can be understood in terms of the concentration of PEG in the water (Table 1). For example, the 30% free PEG suspension had an effective polymer concentration of 5.4 mg/mL surrounding the particles compared to the 18 mg/mL concentration of adsorbed PAA-PEO comb-polymer. In a previous study it was found through UV-Vis spectroscopy that less than 5% of the PAA-PEO chains do not adsorb to particles [19].

Table 1: Concentrations of free PEG chains as a percentage of the weight % of the adsorbed PAA-PEO.

Amount of free PEG by weight of the adsorbed PAA-PEO (%)	10	20	30	40	50
Concentration of free PEG in water (mg/mL)	1.8	3.6	5.4	7.2	9.0

Rheometry Tests

Rheometry was applied to examine the behavior of the suspension under flow as an analog for the processing conditions of MgO suspensions with an Anton Paar MCR 302 rheometer. Previously wall slip was discovered to greatly modify the viscosity readings when suspensions were tested in a rheometer coupled with *in situ* ultrasonic velocimetry [22]. To obtain accurate rheometry measurements by minimizing wall slip, a vane fixture was used along with a roughened cup. Pre-shear was applied for 30 s at 500 s^{-1} followed by a 10 s pause before starting the rheometry tests to allow residual stresses to relax from the pre-shear and then start the measurement with the suspensions having the same strain history. Viscosity curves were used to examine the viscosity and shear stress of the suspensions over ramped shear rate from 0.01 to 100 s^{-1} for 300 seconds. Shear start-up tests at the constant shear rate of 0.1 s^{-1} revealed the time-dependent viscosity for 200 s to provide insights to how the suspension responded to mixing. Creep tests with an applied shear stress of 15 Pa measured shear rate for 500 s as an assessment of the suspensions' resistance to flow as a simulation of pipe flow.

In addition to shear rheometry, ultrasonic speckle velocimetry (USV) measurements were carried out with a custom-made USV system coupled to a TA Instruments ARG2 rheometer. Due to insufficient ultrasonic scattering for the 0.33 weight percent sample(s), the suspension weight ratio of water to MgO was adjusted from 0.33 to 0.42 (solid volume fraction of 0.40). The weight ratio change was completed to give optimal ultrasonic speckle signal from the MgO particles, in particular to avoid too strong multiple scattering of the ultrasound. All added polymer concentrations were adjusted according to the weight percentage of particles to match prior experiments. Shear start-up tests at 10 s^{-1} were performed in a Taylor-Couette (i.e. concentric cylinder) geometry to observe the macroscopic flow behavior, and to quantify the velocity profile across the thickness of the sample within the gap size (2 mm) of the Couette cell. More details on the experimental technique and on USV measurements can be found in [23].

Additional Suspension Characterization

The volume of sediment to the volume of separated water (supernatant) was measured throughout the sedimentation of the suspensions over 7 days. Graduated cylinders were used to measure the volume of water to sediment with periodic recordings. A Nanosizer nano-z (Malvern Instruments) was used to measure the zeta potential of 0.01 wt % MgO solutions with and without 0.01 wt % polymer solutions. Samples were stirred for 24 hours, sonicated for 5 minutes and stirred for 2 minutes and allowed to equilibrate at 25° C for one minute before 3 cycles of 50 runs were measured and averaged [19]. Dynamic light scattering (DLS) was performed with a Nanosizer nano-z (Malvern Instruments) to determine the hydrodynamic radii of PAA-PEO and PEG at 5 mg/mL. Samples were stirred for 30 minutes and equilibrated at 25° C for one minute before three measurements of 10 runs each were conducted and averaged.

RESULTS AND DISCUSSION

Zeta Potential Measurements

Measuring the zeta potential of MgO in relationship to PEG and PAA-PEO serves as a general indicator of adsorption via electrostatic attraction, measured at the slip plane. During these experiments the pH was monitored to demonstrate that the MgO mixture was below the isoelectric point, for MgO that is about 12.45 [4]. The pH with MgO and deionized water with and without the addition of polymers was consistently in the range of 9.8 – 10.95. Therefore, the MgO always maintained a positive zeta potential [4,24] as referenced in Table 2 below. The values in Table 2 are averaged from 3 samples tested, and each zeta potential test cycled 3 times with 50 runs. The peaks were averaged and the standard deviation was calculated during post data processing.

Table 2: Zeta potential results

Material	MgO	PAA-PEO	PEG	PAA-PEO + PEG
Zeta Potential (mV)	22	-13.7	15.9	-11.47
Standard Deviation (mV)	0.75	0.36	3.76	1.43

As PAA-PEO was added to the MgO suspension, both the magnitude and sign changed in the zeta potential, indicating a charge screen at the slipping plane due to electrostatic adsorption mechanisms [4,19]. The surface charge, referenced in Table 2, of MgO was 22 mV with a standard deviation of 0.75 mV; once the PAA-PEO was added, the potential changed to –13.7 mV with a standard deviation of 0.36 mV. However, when only adding PEG with MgO, no significant reduction in the zeta potential was observed. Results from the literature show that oxides, such as MgO, do not possess the necessary Bronsted acid sites for adsorption to occur with the ether oxygen for induced hydrogen bonding, which have been found to be the dominating mechanism that causes adsorption of PEG and PEO onto oxide surfaces [24]. Therefore, even though the zeta potential magnitude differs with PEG, shown in Table 2, the onsets of electrostatic adsorption between the MgO surface and PEG are negligible unless Bronsted acidic sites are present on the oxide surface to induce hydrogen bonding [24–26]. These results imply that PEG does not have any significant adsorption and can be studied as a “free” polymer within the MgO-PAA-PEO suspensions. Further, addition of the PAA-PEO and PEG solutions into the MgO mixture, showed a magnitude and sign change in the zeta potential that was similar to that of the MgO – PAA-PEO measurement, referenced in Table 2. Thus showing further evidence, that adsorption of PEG is negligible on the MgO surface.

Additionally, the total organic carbon (TOC) results from a previous study of stabilized cementitious suspensions are consistent with the zeta potential measurements. PAA-PEO had 91.9% adsorption to MgO particles when added at a concentration of 2.7 mg/mL with higher concentrations having more adsorption than lower concentrations [27].

Additional characterization of PEG and PAA-PEO

Dynamic light scattering revealed a hydrodynamic radius of 2.09 nm for free PEG, which is on [28]. A hydrodynamic radius of 2.57 nm was measured for the PAA-PEO comb-polymers. Aggregation of the PEG chains in solution is deemed unlikely for the suspensions due to the size scale similarity of DLS results with scaling law predictions for a single polymer chain in solution. It should be noted that the 1,000 g/mol PEG is not capable of chain entanglement due to the low molecular weight [28]. Aqueous PEG solutions were found to be Newtonian for the 10-50 weight % free PEG concentrations used for the suspensions, which is expected due to the low PEG molecular weight [29,30]. Therefore it is believed that the free PEG chains did not entangle or overlap due to the concentrations remaining less than the overlap concentration (~9.2 vol% calculated with equation from [16] based on 1,000 g/mol with a density of 1.1 g/cm^2 and the measured hydrodynamic radius).

Suspensions with adsorbed PAA-PEO and free PEG chains

Viscosity curves served as an analog for mixing with viscosity increases and decreases over different shear rates indicating either aggregation or dispersion in the concentrated colloidal suspensions [31]. Shown in Figure 1a, viscosity curves for suspensions with both adsorbed PAA-PEO and free PEG had varied viscosities over ramped shear rate. Additions of 10 to 30 weight % free PEG (by weight of PAA-PEO) to the suspensions led to viscosities ~5-10 Pa-s above the control suspension, whereas even higher free PEG concentrations of 40 and 50% resulted in ~10 Pa-s lower viscosities for shear rates between 0.1 and 1 s^{-1} (Figure 1a). Shear start-up tests (Figure 1b) with a constant applied shear rate of 0.1 s^{-1} demonstrated corresponding trends with 10, 20, and 30% free PEG suspensions having larger overshoot height (difference between local maximum and local minimum) and 40 and 50% free PEG maintaining the lowest viscosities of the six suspensions. The presence of an overshoot in start-up tests may denote particle network formation [19], and a larger overshoot height signifies a greater degree of flocculation [32]. Of the six samples, the 30 weight % free PEG has the greatest viscosity from the viscosity curve as well as the largest peak height from the start-up test. Increases in viscosity and shear stress over time seen in the start-up tests (Figure 1b) are likely due to aging long before the onset of sedimentation at longer times.

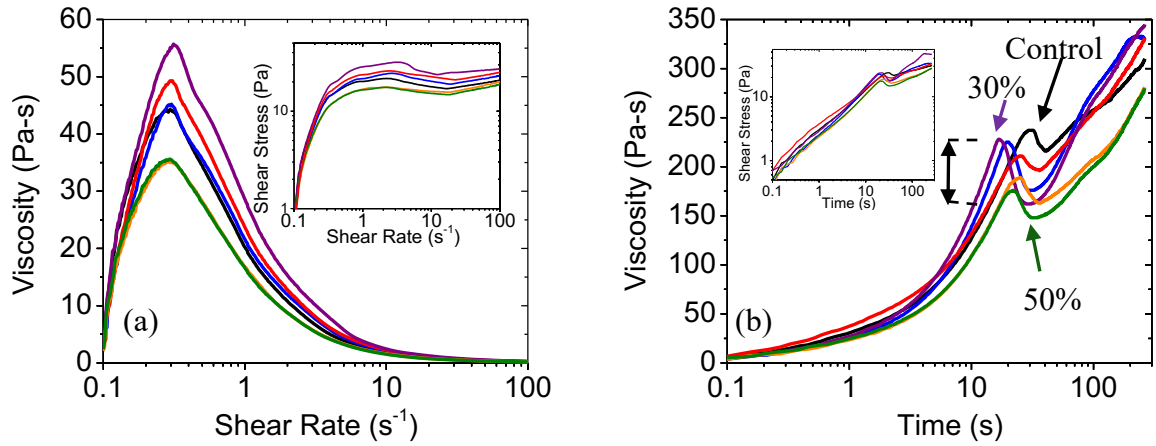

Figure 1: Viscosity curves with PAA-PEO with shear stress insert (a) and shear start-up tests at 0.1 s^{-1} (b) for 0 (black), 10 (blue), 20 (red), 30 (purple), 40 (orange), and 50 (green) % free PEG with shear stress insert. The overshoot height for the 30% free PEG suspension is displayed with the black arrow.

Depletion flocculation is hypothesized to be the mechanism for the increased viscosity of the 10, 20, and 30% free PEG suspensions with adsorbed PAA-PEO. Aggregation of the particles (and the resulting viscosity increase) may have occurred due to osmotic pressure differences from free chains concentration gradients promoting stronger osmotic-driven attraction between neighboring particles [31]. Furthermore, the presence of the steric PEO side-chains from the particle surfaces may have been sufficient to prevent depletion flocculation [33,34]. Computational studies have found that depletion forces can override steric stabilization when the free chains have the same chemistry as the steric chains with the same or shorter molecular weights [35]. These theories have also been attributed to micron-scale systems. Depletion has been reported to flocculate vesicles [36] and lipid bilayers [36] and as well as ~1 μm particles having more depletion aggregation than nano-sized particles [15], making it a viable situation for cementitious concentrated suspensions. The hypothesized depletion aggregation of the 10-20% free PEG is shown in Figure 2a, followed by the transition point concentration of 30% in Figure 2b. Figure 2c displays a representation of depletion stabilization for the 40 and 50% free PEG suspensions.

The stark change to viscosity-reduction at 40 weight % free PEG suggests that depletion attraction diminished with higher concentrations of free polymer. With a greater density of PEG surrounding the particles, it was likely that osmotic attraction transitioned to repulsion on account of the PEG chains serving as an effective steric barrier between particles (Figure 2c). This depletion stabilization has been theorized by Napper (Napper, 1983) and observed to keep colloids and latexes stable only once free polymer concentrations have surpassed a critical level [15,34,37]. Depletion stabilization has been reported to decrease viscosity in nanoscale colloids [38] and the same phenomena correlates to the reduced viscosities of the 40 – 50% free PEG suspensions shown in Figure 1a. Further, with additions of high concentrations of free polymer it

was probable that free PEG chains keep uniform distances from each other and that even greater concentrations of free PEG would result in free PEG and particle phase separation [15].

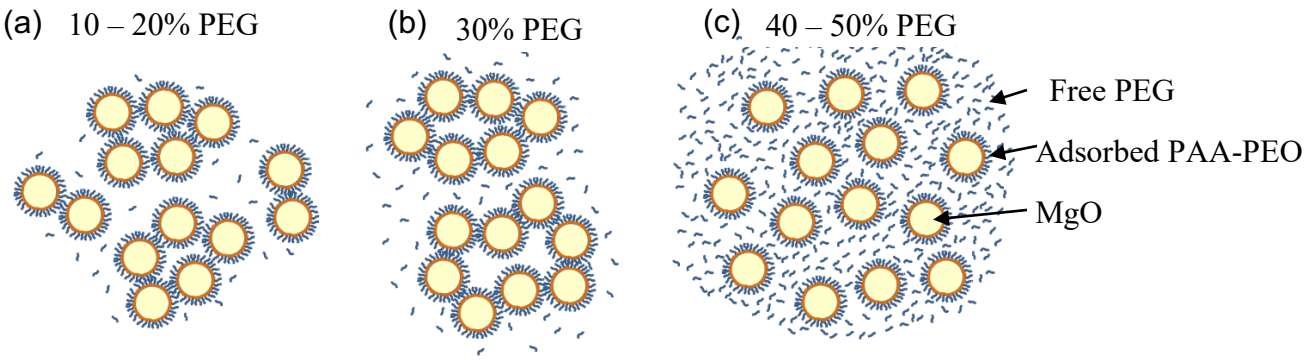

Figure 2: Schematic representation (MgO not drawn to scale) of the hypothesized particle behaviors due to (a) depletion attraction between particles, (b) increased depletion flocculation, and (c) depletion stabilization.

Flow resistance under applied shear stress (i.e., creep tests) was evaluated as an indication of ease of pipe flow. Measured shear rates from the applied shear stress tests (Figures 3a and 3b) showed 30% free PEG with the lowest measured shear rates on the order of 10-20 s^{-1} and 50% free PEG (not shown) as having no flow under 15 Pa applied shear stress. The hierarchy of creep flow results support the three different flow regimes based on the concentration of free PEG: a region of viscosity increase with moderate ease of flow (10 and 20% free PEG), a surge in the viscosity with increased flow resistance (transition point) (30%), and a viscosity-reducing section with varied ease of flow (40 % free PEG).

Although the 50% free PEG suspension displayed the lowest viscosity (Figures 1a and 1b), it did not flow in the creep test and is not shown in Figure 4 due to the small measured shear rates ($<<$ 1 s^{-1}). This finding imparts an important trade-off between the addition of high concentrations of free chains for lower viscosity (from depletion stabilization) and the increase to the resistance of applied stresses, acting as an effective increase in yield stress [31]. The contrasting flow behavior between the low-viscosity curve and low shear rate observed in the creep test may be due to different rearrangements of the free chains and particles upon applying the shear stress rather than the shear rate [31]. During the creep test the internal microstructure of the suspension may deform with particle rearrangements that are different from the break-up of aggregates under applied shear rate [39]. For construction applications, it should be considered if either ease of mixing or pumping is more desirable before selecting a depletion-stabilizing PEG concentration as an additional additive for cementitious pastes.

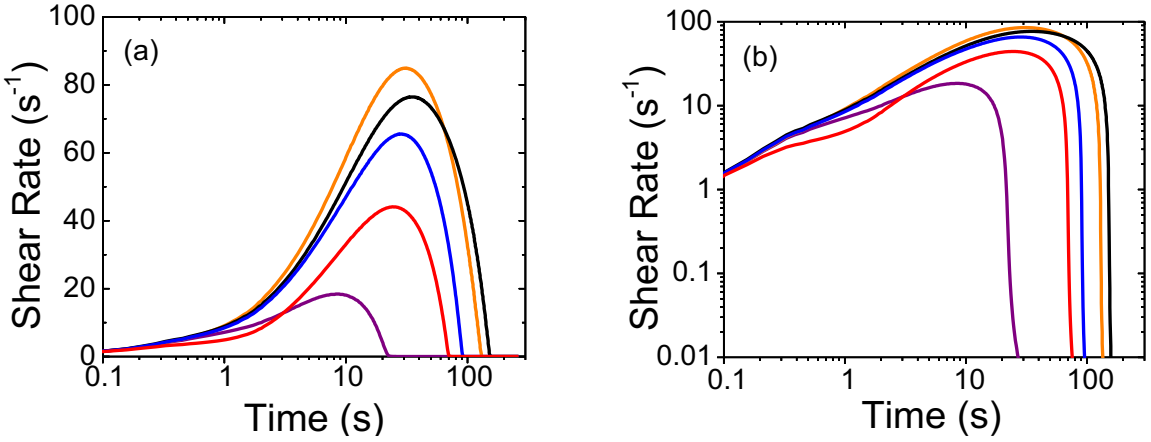

Figure 3: Creep tests at 15 Pa applied shear stress with PAA-PEO for 0 (black), 10 (blue), 20 (red), 30 (purple), and 40 (orange) % free PEG shown in semi-log (a) and log-log scale (b); it should be noted that the 50% free PEG suspension did not flow at 15 Pa.

Suspensions containing free PEG without adsorbed PAA-PEO

For comparison, suspensions without adsorbed PAA-PEO were tested to examine the rheological impact of the free PEG alone on suspension fluidity. The viscosity curves of the MgO and free PEG had an order of magnitude lower viscosities over all shear rates than those with PAA-PEO, which is believed to be caused by sedimentation of the particles before and during shear. Start-up tests also demonstrated signs of sedimentation with decreased viscosities while creep measurements had greater shear rates at lower applied shear stress. Such rapid sedimentation during testing created a water supernatant phase above the sediment that was seen after testing and is most likely be the cause of the low viscosities and high shear rates observed for samples without PAA-PEO. From these findings it may be deducted that adsorbed comb-polymer is required to obtain the depletion and steric stabilization of free chains and to prevent rapid particle sedimentation under shear.

Sedimentation Studies

Sedimentation studies gave insights to the particle-polymer interactions through comparing the rate of particle settling and the final supernatant volume between suspensions with and without adsorbed PAA-PEO. Shown in Figure 4, the volume of supernatant separated from the sediment to total volume are given for suspensions with 10 – 50% free PEG with and without PAA-PEO, with increased supernatant volume indicating greater separation of the particles from the water phase.

Sedimentation of the suspensions with adsorbed PAA-PEO do not display much variance in the supernatant volume to the total volume at long time (0.06 – 0.08) (Figure 4a) whereas suspensions without PAA-PEO have a wide range of supernatant volume to total volume (0.05 – 0.15) (Figure 4b). Additionally, suspensions without PAA-PEO had more rapid sedimentation

than those with PAA-PEO. Figure 4a has an increased time range for sedimentation onset (76 - 1383 min) while the suspensions without PAA-PEO begin sedimentation as early as 5 min and at most 158 min (Figure 4b). The faster sedimentation and wider range of supernatant volumes for the bare suspensions with free PEG is believed to be due to the lack of both depletion and steric particle stabilization. For suspensions with PAA-PEO, steric stabilization provided by the adsorbed PAA-PEO reduced the likelihood of particle aggregation and kept particles apart although the effect of gravity eventually overcame the steric repulsion, leading to sedimentation at long times (Napper, 1983). The concentration of free PEG had little effect on the sedimentation behavior in the presence of the adsorbed PAA-PEO. On the contrary, suspensions without PAA-PEO displayed no significant stabilization and therefore were prone to van der Waals attraction which may have assisted sedimentation through the formation of aggregates that sediment faster due to the pull of gravity (Napper 1983,Autier, Azéma, & Boustingorry, 2014). This phenomenon may be responsible for the large increase in supernatant volume around 100 minutes seen in Figure 4b. It is believed that suspensions without PAA-PEO sediment more rapidly during rheometry tests (which were 5 – 10 minutes on average) than sedimentation tests due to stimulus by the hydrodynamic force of the shear [31].

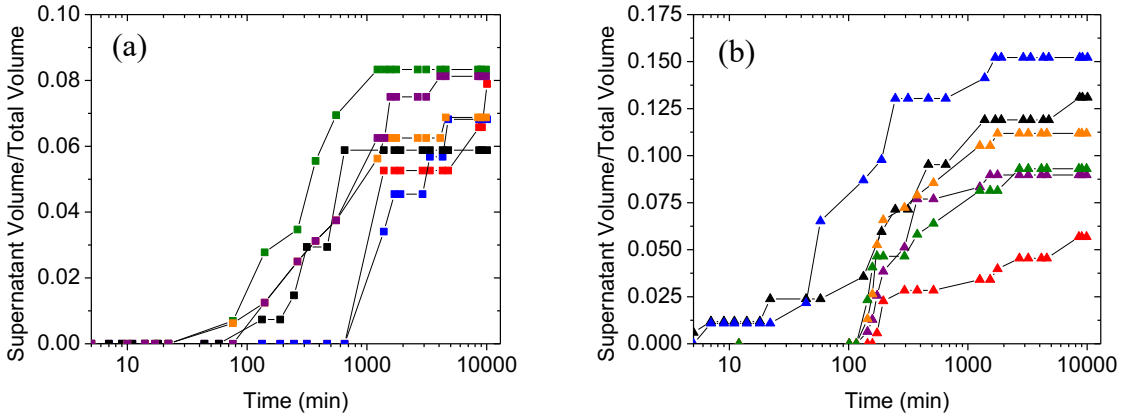

Figure 4: Sedimentation results for suspensions with PAA-PEO (a) and without PAA-PEO (b) for 0 (black), 10 (blue), 20 (red), 30 (purple), 40 (orange), and 50 (green) % free PEG by weight of PAA-PEO.

Ultrasonic speckle velocimetry (USV) for *insitu* flow visualization

The impact of adsorbed PAA-PEO on suspension lubrications was investigated with 0.42 water: MgO weight ratio model suspensions (for optimal ultrasonic speckle signal) with 20 and 50% free PEG based on the weight percent of PAA-PEO. Figure 5 displays the average velocity profiles of the suspensions with adsorbed PAA-PEO during the steady-state portion of start-up test at 10 s^{-1} between 10 and 100 s. The initial velocities between 0 - 10 s were disregarded due to the time needed for the TA ARG2 rheometer to reach the 10 s^{-1} shear rate. These averaged

velocity profiles demonstrate the dominant flow behaviors in the suspension over the 10-100 s testing period, which include wall slip, plug flow, and shear banding.

For both 0 and 20% PEG with PAA-PEO, shear banding – regions of the sample that portray different shear rates than other regions of the sample [41] – is evident by the kink in the velocity profiles (Figures 5a and 5b). Further, the 20% free PEG suspension may not have contained enough PEG to significantly deviate from the shear banding behavior of the 0% PEG suspension. A strikingly different flow pattern emerged in the 50% PEG suspension with a nearly constant velocity region next to the shear band at ~0.75 mm (Figure 5c). This feature is an indication of plug flow, which is a near-zero shear rate of the material in the center of the gap while lubricating layers at the walls are sheared with a large velocity gradient [42]. Plug flow has been reported to exist in concrete pumping through pipes with mortar-based lubrication layers along the pipe walls [43–46]. The plug flow observed in the suspension with adsorbed PAA-PEO and 50 % free PEG suggests that lubrication not only occurred from the PAA-PEO but was also increased by the presence of free PEG.

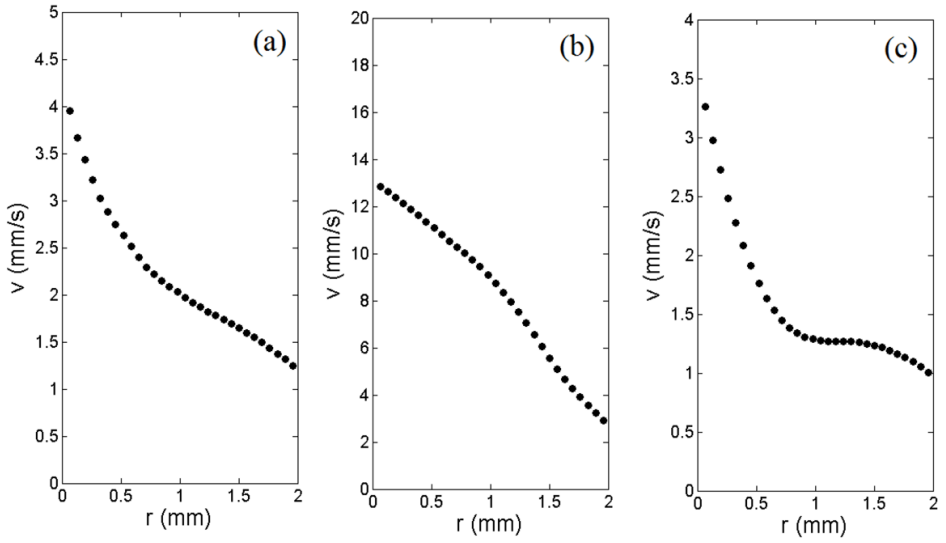

Figure 5: USV particle velocity profiles for MgO suspensions with PAA-PEO for 0% (a), 20% (b), and 50% PEG by weight of PAA-PEO (c). r = 0 indicates the moving wall surface of the Taylor-Couette fixture and r = 2 mm indicates the stationary surface of the outer cylindrical cup of the fixture. The shear rate is 10 s^{-1} and the corresponding velocity of the rotating cylinder is 20 mm/s.

USV velocity profiles shown in Figure 6 of bare MgO (Figure 6a) and suspensions with 20 (Figure 6b) and 50% PEG (Figure 6c) without PAA-PEO are mostly linear. In Figure 6a a small shear band is displayed close to the stationary cylinder but without plug flow. Due to the rapid sedimentation of the suspensions without PAA-PEO, a sufficient lubrication layer may not have formed. The slight shear banding observed in suspensions without PAA-PEO resulted in two

different shear rate zones in the gap, which may have separate contributions to lubrication that are not as significant as the plug flow seen in the suspension with 50% free PEG and adsorbed PAA-PEO.

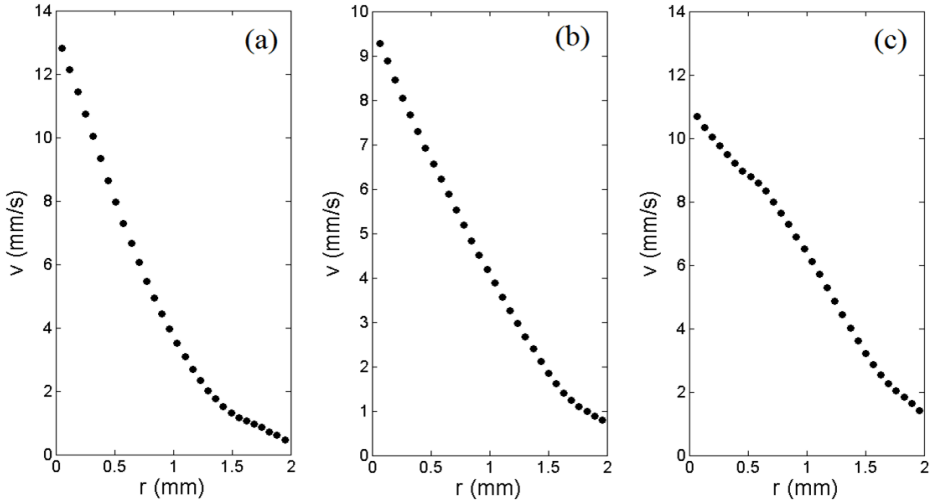

Figure 6: USV particle velocity profiles for MgO suspensions without PAA-PEO and 0% (a), 20% (b), and 50% PEG by weight of PAA-PEO (c). Other parameters are those of Figure 5.

In addition to non-linear velocity profiles, suspensions have been documented for their tendency to wall slip during rheometry experiments [41–43] in which the sample does not rotate at the angular velocity of the moving wall but rather moves at a slower velocity than prescribed by the applied shear rate [38,44–46]. The effective magnitude of wall slip at the moving wall is calculated here as the velocity of the moving wall (v_0 = 20 mm/s at 10 s^{-1}) minus the flow velocity measured along the moving wall (taken from the velocity profiles shown in Figures 5 and 6 at r~0) divided by v_0 and averaged over time. The effective wall slip magnitude and the effective viscosities recorded by the rheometer for each USV suspension experiment during 10 – 100 s of the 10 s^{-1} start-up test are shown in Table 3. Wall slip and viscosities measured from 0 -10 s were not analyzed due to the ARG2 rheometer requiring a few seconds to reach the desired shear rate for the suspensions to reach the desired shear rate of 10 s^{-1}.

Table 3: Average Wall Slip and Viscosities of USV suspensions for 10-100 s

Suspension	0% PEG, no PAA-PEO	20% PEG, no PAA-PEO	50% PEG, no PAA-PEO	0% PEG with PAA-PEO	20% PEG with PAA-PEO	50% PEG with PAA-PEO
Average Wall Slip (%)	35.0	55.0	47.5	80.0	35.0	82.5
Apparent Viscosity (Pa-s)	0.087	0.124	0.151	0.155	0.138	0.181

The suspensions without free PEG but with PAA-PEO had strong wall slip at the moving wall (80%, see Table 3), which may have resulted from the steric-induced particle dispersion. Wall slip was even greater for PAA-PEO with 50% free PEG (82.5%), in which potential lubrication layers formed at the wall may better facilitate plug flow (Figure 5c). These two suspensions with high wall slip are hypothesized to have friction-reducing lubricating layers [22,47] that enables ease of flow along both the moving and stationary walls of the rheometer fixture. Near-wall lubrication in the 50% PEG with PAA-PEO suspension may be a result of the depletion stabilization that reduces particle aggregation, which is consistent with the low-viscosity rheology data seen in Figure 1a. Likewise, near-wall lubrication in the 20% PEG with PAA-PEO (35% wall slip) suspension may be attributed to the depletion flocculation (increased viscosity, Figure 1a) resulting in particle clusters that increase friction instead of lubrication [48]. However, the thickness of lubrication layers along the walls is not discernible with USV due to the ~50 μm spatial resolution of the technique. Further, we note that although wall slip is reported here in terms of the velocity at the moving wall, the stationary wall of the 0 and 50% PEG suspensions also maintained significant levels of wall slip.

Average viscosities of the suspensions with adsorbed PAA-PEO (0.138 – 0.181 Pa-s) do not reflect the trends observed in the viscosity curves of Figure 1 due to the long times of the USV start-up tests and the differences in their water to MgO ratios. Furthermore, the wall slip distorts the apparent viscosity such that the measured values do not reflect the actual properties of the suspensions. Absence of PAA-PEO in other suspensions enabled sedimentation (which resulted in the low measured viscosities ranging from 0.087-0.151 Pa-s) due to the lack of particle dispersion and therefore suspensions without PAA-PEO are less likely to have developed near-wall lubrication layers.

Lubrication forces may have assisted the suspension flow through the presence of free PEG reducing particle gliding friction. Either mediated by depletion flocculation or brought about by hydrodynamic shearing forces, particle clusters may form without significant interaction with each other until the concentration of clusters reaches a percolation threshold and their collisions

result in shear thickening [31]. As a counteraction to the flow impedance of aggregates, lubrication typically stems from water ordering [49] around the PCE, which acts as a gliding plane for particles to slip past each other with reduced friction [2]. Free PEG chains may also have reduced the water surface tension and therefore created lubricating zones around particles or particle aggregates as well as in the vicinity of the wall of the rheometer fixture. Lubrication layers near the fixture walls typically consist of a locally reduced particle concentration that maintains a faster shear rate than the material in the middle of the gap [43]. Additionally, near-wall lubrication has been reported to occur during cement pumping [43–46] and is believed to contribute to wall slip through the reduced friction between the sample and the rotating wall [22,50].

Conclusions

The rheological influence of free PEG among PAA-PEO comb-polymers that adsorbed onto the MgO particle surface was analyzed to determine the role of non-adsorbing PEG in manipulating the viscosity of model cementitious suspensions. Rheometry tests delineated the role of free PEG as a concentration-dependent aggregation initiator or particle dispersant based on osmotic pressure driven depletion. Free PEG potential processing behavior was deemed to be viscosity reducing for 40 and 50% free PEG but with 50% increasing the resistance to initial flow in creep measurements. High concentrations of free chains may rearrange under applied pressure, unlike during viscosity curves under an imposed shear rate, which may restrict their ability to flow easily during pipe flow. Concentrations of 10 to 30% free PEG were believed to have depletion flocculation due to increased viscosities and the large peaks seen in start-up tests. Suspensions without PAA-PEO were found to sediment during testing. Sedimentation test results also supported the conclusion that PAA-PEO is necessary for particle dispersion due to the similarities in the PAA-PEO stabilized suspensions sedimentation rates regardless of the free PEG concentration.

The lubricating potential of free PEG on suspensions was monitored with USV rheometry to assess the impact of free PEG on wall slip and velocity profiles. The suspension with PAA-PEO and 50% free PEG demonstrated the most wall slip out of the suspensions tested and was the only suspension tested to demonstrate plug flow. PAA-PEO suspensions without PEG displayed the second greatest magnitude of wall slip which may be induced by steric stabilization. Wall slip and plug flow are believed to be indications of effective lubrication layers that helped the suspension flow along confined walls at reduced applied shear stresses. PAA-PEO was reasoned to be essential for significant lubrication, as suspensions without PAA-PEO did not demonstrate as much wall slip or plug flow and sedimented rapidly. The beneficial lubrication of PAA-PEO and PEG at high free PEG concentrations may further improve cement pipe flow.

Based on the transition from aggregation to stabilization for suspensions containing free PEG chains, it is suggested that the cement industry may benefit from exploring the addition of PEG as a supplement to adsorbed superplasticizers. Addition of 30% free PEG may be a transition point, in which 40% free PEG can lead to reduced viscosities through dispersing particles and

20% free PEG may result in viscosity-increasing aggregation. Furthermore, the use of PAA-PEO with free PEG fosters the formation of lubrication layers which allow for greater ease of mixing and pumping seen in the increased wall slip. Caution should be taken to assess the flow behavior of systems with free chains under applied shear stresses, as high concentrations of free chains may lead to resistance to flow. Although the advantages of depletion-stabilizing free chains is desirable, it should be noted that free chains without adsorbed superplasticizer may cause significantly more sedimentation than the suspensions with adsorbed chains on account of supernatant viscosity differences.

Acknowledgements

The work conducted herein is supported by the National Science Foundation Graduate Research Fellowship Program under Grant No. DGE-1333468. C.P. and S.M. acknowledge funding from Institut Universitaire de France and from the European Research Council under the European Union's Seventh Framework Programme (FP7/2007-2013) and ERC Grant Agreement No. 258803.

References

1. Bedrov D, Smith GD, Chun BW. Influence of poly(ethylene oxide) brushes on the rheological properties of MgO colloidal suspensions in water. *Eur Polym J*. 2010;46(11):2129-2137. doi:10.1016/j.eurpolymj.2010.08.007.
2. Ferrari L, Kaufmann J, Winnefeld F, Plank J. Multi-method approach to study influence of superplasticizers on cement suspensions. *Cem Concr Res*. 2011;41(10):1058-1066. doi:10.1016/j.cemconres.2011.06.010.
3. Flatt RJ, Martys NS, Bergström L. T he Rheology of Cementitious Materials. 2004;29(5):314-318.
4. Houst YF, Bowen P, Perche F, et al. Design and function of novel superplasticizers for more durable high performance concrete (superplast project). *Cem Concr Res*. 2008;38(10):1197-1209. doi:10.1016/j.cemconres.2008.04.007.
5. Kjeldsen AM, Flatt RJ, Bergstr??m L. Relating the molecular structure of comb-type superplasticizers to the compression rheology of MgO suspensions. *Cem Concr Res*. 2006;36(7):1231-1239. doi:10.1016/j.cemconres.2006.03.019.
6. Mehta PK, Monteiro PJM. Concrete: microstructure, properties, and materials. *Concrete*. 2006:684. doi:10.1036/0071462899.
7. Mehta PK, Monteiro PJM. Concrete: microstructure, properties, and materials. *Concrete*. 2006:684. doi:10.1036/0071462899.
8. Flatt RJ, Schober I, Raphael E, Plassard C, Lesniewska E. Conformation of adsorbed comb copolymer dispersants. *Langmuir*. 2009;25(2):845-855. doi:10.1021/la801410e.
9. Flatt RJ, Houst YF. A simplified view on chemical effects perturbing the action of superplasticizers. *Cem Concr Res*. 2001;31(8):1169-1176. doi:10.1016/S0008-8846(01)00534-8.
10. Laarz E, Kauppi A, Andersson KM, Kjeldsen AM, Bergstr??m L. Dispersing multi-component and unstable powders in aqueous media using comb-type anionic polymers. *J Am Ceram Soc*. 2006;89(6):1847-1852. doi:10.1111/j.1551-2916.2006.01055.x.
11. Frith WJ. Shear thickening in model suspensions of sterically stabilized particles. *J Rheol (N Y N Y)*. 1996;40(4):531. doi:10.1122/1.550791.
12. Jayasree C, Murali Krishnan J, Gettu R. Influence of superplasticizer on the non-Newtonian characteristics of cement paste. *Mater Struct*. 2011;44(5):929-942. doi:10.1617/s11527-010-9677-6.
13. Jayasree C, Gettu R. Experimental study of the flow behaviour of superplasticized cement paste. *Mater Struct*. 2008;41(9):1581-1593. doi:10.1617/s11527-008-9350-5.
14. Hot J, Bessaies-Bey H, Brumaud C, Duc M, Castella C, Roussel N. Adsorbing polymers and viscosity of cement pastes. *Cem Concr Res*. 2014;63(October 2012):12-19. doi:10.1016/j.cemconres.2014.04.005.
15. Liang W, Tadros TF, Luckham PF. Flocculation of Sterically Stabilized Polystyrene Latex Particles by Adsorbing and Nonadsorbing Poly(acrylic acid). *Langmuir*. 1994;10(2):441-446. doi:10.1021/la00014a018.

16. Heath D, Tadros T. Rheological Investigations of the Effect of Addition of Free Polymer to Concentrated Sterically Stabilised Polystyrene Latex Dispersions. *Faraday Discuss Chem Soc*. 1983;76:203-218.

17. Tuinier R, Fan TH, Taniguchi T. Depletion and the dynamics in colloid-polymer mixtures. *Curr Opin Colloid Interface Sci*. 2015;20(1):66-70. doi:10.1016/j.cocis.2014.11.009.

18. Sozanski K, Wisniewska A, Piasecki T, et al. A depletion layer in polymer solutions at an interface oscillating at the subnano- to submicrometer scale. *Soft Matter*. 2014;10(39):7762-7768. doi:10.1039/c4sm01280a.

19. Murray LR, Erk KA. Jamming rheology of model cementitious suspensions composed of comb-polymer stabilized magnesium oxide particles. *J Appl Polym Sci*. 2014;131(12):1-11. doi:10.1002/app.40429.

20. Luo Y, Ran Q, Wu S, Shen J. Synthesis and characterization of a poly(acrylic acid)-graft-methoxy poly(ethylene oxide) comblike copolymer. *J Appl Polym Sci*. 2008;109(5):3286-3291. doi:10.1002/app.28272.

21. Banfill PFG. Rheology of Fresh Cement and Concrete. *Rheol Rev*. 2006;2006:61-130. doi:10.4324/9780203473290.

22. Manneville S, Becu L, Colin A, Bécu L. High-frequency ultrasonic speckle velocimetry in sheared complex fluids. *Eur Phys J Appl Phys*. 2004;28(3):361-373. doi:10.1051/epjap:2004165.

23. Gallot T, Perge C, Grenard V, Fardin MA, Taberlet N, Manneville S. Ultrafast ultrasonic imaging coupled to rheometry: Principle and illustration. *Rev Sci Instrum*. 2013;84. doi:10.1063/1.4801462.

24. Mathur S, Moudgil B. Adsorption Mechanism(s) of Poly(Ethylene Oxide) on Oxide Surfaces. *J Colloid Interface Sci*. 1997;196(196):92-98. doi:10.1006/jcis.1997.5192.

25. Walker WJ, Reed JS, Verma SK, Zirk WE. Adsorption behavior of poly(ethylene glycol) at the solid/liquid interface. *J Am Ceram Soc*. 1999;82(3):585-590. isi:000079374400013.

26. Bouhamed H, Boufi S, Magnin A. Alumina interaction with AMPS-MPEG random copolymers: I. Adsorption and electrokinetic behavior. *J Colloid Interface Sci*. 2003;261(2):264-272. doi:10.1016/S0021-9797(03)00100-0.

27. Murray LR, Gupta C, Washburn NR, Erk KA. Lignopolymers as viscosity-reducing additives in magnesium oxide suspensions. *J Colloid Interface Sci*. 2015;459:107-114. doi:10.1016/j.jcis.2015.07.037.

28. Rubinstein M, Colby RH. Polymer physics. *Polym Int*. 2003:440. doi:10.1002/pi.1472.

29. Teraoka I. *Polymer Solutions: An Introduction to Physical Properties*. Vol 3.; 2002. doi:10.1002/0471224510.

30. Khandavalli S, Rothstein JP. Extensional rheology of shear-thickening fumed silica nanoparticles dispersed in an aqueous polyethylene oxide solution. *J Rheol (N Y N Y)*. 2014;58(2):411-431. doi:10.1122/1.4864620.

31. Wagner N, Mewis J. Colloidal Suspension Rheology. *J Chem Inf Model*. 2013;53(9):1689-1699. doi:10.1017/CBO9781107415324.004.

32. Burns JL, Yan Y De, Jameson GJ, Biggs S. The rheology of concentrated suspensions of

depletion-flocculated latex particles. *Colloids Surfaces A Physicochem Eng Asp*. 2003;214(1-3):173-180. doi:10.1016/S0927-7757(02)00388-6.

33. Larson RG. *The Structure and Rheology of Complex Fluids*.; 1999. doi:10.1029/2006EO230009.

34. Kirby G, Lewis JA, Matsuyama H, Morissette S, Young JF. Polyelectrolyte effects on the rheological properties of concentrated cement suspensions. *J Am Ceram Soc*. 2000;83:1905-1913.

35. Dutta N, Green D. Nanoparticle stability in semidilute and concentrated polymer solutions. *Langmuir*. 2008;24(10):5260-5269. doi:10.1021/la7027516.

36. Kuhl T, Guo Y, Alderfer JL, et al. Direct Measurement of Polyethylene Glycol Induced Depletion Attraction between Lipid Bilayers. *Langmuir*. 1996;12(12):3003-3014. doi:10.1021/la9508021.

37. Ogden AL, Lewis JA. Effect of Nonadsorbed Polymer on the Stability of Weakly Flocculated Suspensions. *Langmuir*. 1996;7463(7):3413-3424. doi:10.1021/la950953o.

38. Kim S, Hyun K, Moon JY, Clasen C, Ahn KH. Depletion stabilization in nanoparticle-polymer suspensions: Multi-length-scale analysis of microstructure. *Langmuir*. 2015;31(6):1892-1900. doi:10.1021/la504578x.

39. Coussot P, Tabuteau H, Chateau X, Tocquer L, Ovarlez G. Aging and solid or liquid behavior in pastes. *J Rheol (N Y N Y)*. 2006;50(May 2015):975-994. doi:10.1122/1.2337259.

40. Autier C, Azéma N, Boustingorry P. Using settling behaviour to study mesostructural organization of cement pastes and superplasticizer efficiency. *Colloids Surfaces A Physicochem Eng Asp*. 2014;450(1):36-45. doi:10.1016/j.colsurfa.2014.02.050.

41. Salmon J-B, Colin A, Manneville S, Molino F. Velocity profiles in shear-banding wormlike micelles. *Phys Rev Lett*. 2003;90(June):228303. doi:10.1103/PhysRevLett.90.228303.

42. Divoux T, Barentin C, Manneville S. Stress overshoot in a simple yield stress fluid: An extensive study combining rheology and velocimetry. *Soft Matter*. 2011;7:9335. doi:10.1039/c1sm05740e.

43. Choi MS, Kim YJ, Jang KP, Kwon SH. Effect of the coarse aggregate size on pipe flow of pumped concrete. *Constr Build Mater*. 2014;66:723-730. doi:10.1016/j.conbuildmat.2014.06.027.

44. Choi M, Roussel N, Kim Y, Kim J. Lubrication layer properties during concrete pumping. *Cem Concr Res*. 2013;45(1):69-78. doi:10.1016/j.cemconres.2012.11.001.

45. Jacobsen S, Haugan L, Hammer TA, Kalogiannidis E. Flow conditions of fresh mortar and concrete in different pipes. *Cem Concr Res*. 2009;39(11):997-1006. doi:10.1016/j.cemconres.2009.07.005.

46. Jacobsen S, Cepuritis R, Peng Y, Geiker MR, Spangenberg J. Visualizing and simulating flow conditions in concrete form filling using pigments. *Constr Build Mater*. 2013;49:328-342. doi:10.1016/j.conbuildmat.2013.08.027.

47. Dehmoune J, Manneville S, Decruppe JP. Local velocity measurements in the shear-

thickening transition of dilute micellar solutions of surfactants. *Langmuir*. 2011;27(3):1108-1115. doi:10.1021/la103572c.

48. Heussinger C. Shear thickening in granular suspensions: Interparticle friction and dynamically correlated clusters. *Phys Rev E - Stat Nonlinear, Soft Matter Phys*. 2013;88(5):1-4. doi:10.1103/PhysRevE.88.050201.

49. Israelachvili JN. *Intermolecular and Surface Forces Third Edition*.; 2010. doi:10.1016/B978-0-12-375182-9.10025-9.

50. Divoux T, Tamarii D, Barentin C, Teitel S, Manneville S. Yielding dynamics of a Herschel–Bulkley fluid: a critical-like fluidization behaviour. *Soft Matter*. 2012;8(15):4151. doi:10.1039/c2sm06918k.